Algorithmic Structure of Wind Turbines System based on an Induction Machine Directly Connected to the Grid

Nguyen Huu Nam[1], Prof. Dr. Mytsyk G.S[1,b], Berilov A.V[1,c], Myo Min Thant[1,d]

[1] *Department of Electrical Complexes of Self-Contained Objects and Electrical Transport, National Research University "Moscow Power Engineering Institute", Moscow, Russia.*

Abstract. One of the relatively simple (comparatively cheap) and promising solutions of the wind power plant - the wind turbine system (WTS) with variable speed on the shaft of the wind wheel - is to execute it on the basic of an induction machine - IM. Today, the problem of self-excited induction machine is solved in two ways - by using either capacitors, or electronic converters. As a generating system (based on IM), several WTS are often used, working parallel or directly connected to the grid. For induction machine: squirrel-cage induction generator (SCIG) and doubly-fed induction generator (DFIG) are used, several possible types of them are systematized, evaluated and compared on functional features and properties. Based on computer simulations, the ability of DFIG with back to back converters (in the form of two serially connected 2 level voltage source converters - converter-1 and converter-2) is determined in the rotor circuit at a variable speed of the drive shaft (in modes sub-synchronous and hyper-synchronous speeds) give to the grid only active power. For mass-scale and energy indicators, this structure is the optimum for WTS.

1 Introduction

One of the relatively simple, cheap and promising solutions of the wind turbine system - WTS with variable speed on the shaft of the wind wheel is to execute it on the base of an induction machine - IM. The problem of self-excited induction generator (SCIG) today can be solved by two methods - by using either capacitors or electronic converters. As a generating system - GS (based on IM), several WTS are often used, working either in parallel or connected directly to the industrial network. There are several types of the algorithmic structure of the WTS. In the technical studies, information regarding the physical processes of IM operation in this application (which is necessary for comparing the variants of the WTS, choosing rational algorithmic structure, hence subsequent making competent design, even taking into account, for example, the paper [1,2,3]) is still extremely limited. In order to systematize, preliminary (at least qualitative) comparative assessment and to identify the most promising of algorithmic structure of the WTS, this paper briefly considered the features and properties of several known variants of WTS. In all the considered cases, the generally accepted concept of slip in IM is $s=(\omega_s-\omega_m)/\omega_s$, where ω_s – angular frequency of the voltages and currents of the stator windings; ω_m – angular frequency of the rotor. In this case, the peculiarities of the operation of IM (in the structure of WTS) in two slip zones are considered: in the first zone, sub-synchronous operation, when $s>0$, and in the second zone – hyper-synchronous operation, when $s<0$. Two types of IM are used: a squirrel-cage and a wound rotor with slip rings.

2 Structures of WTS

2.1 WTS with a SCIG

The simplest version of WTS uses a squirrel-cage induction generator (SCIG) [3,4,5,6]. Depending on the design of the IM, various topologies of the power part of the electronic converters are used. In this structure, before connecting the IM to the parallel operation of the WTS (among themselves or to the grid), self-excited IM and stabilization of its voltage at a given level is provided by bank of adjustable capacitors (BC) with a corresponding value of the capacitance C, which varies with the function of the shaft speed and output power of Fig.1. Self-excited IM reaches the point of equality between the voltages on IM windings and capacitors when condition [7] is fulfilled:

$$I_{1C}\,\omega_s\,L_s = I_{1C}/\omega_s C\,, \qquad (1)$$

where I_{1C} - the capacitor current, and L_s - the stator leakage inductance.

From equation (1), the capacitance needed to excite IM at idle mode can be found. With increasing load and decreasing speed, the capacitance value will increase [6]. This simple structure of the WTS during its operation in hyper-synchronous speed (at $s<0$), does not allow full use

© The Authors, published by EDP Sciences. This is an open access article distributed under the terms of the Creative Commons Attribution License 4.0 (http://creativecommons.org/licenses/by/4.0/).

of the wind wheel source due to its inability to transmit the active power of the rotor winding to autonomous load (or the grid). It is transferred to the shaft of the wind wheel, unloading it. This type of WTS is suitable for stand-alone WTS with small power.

When SCIG (in the WTS) is connected directly to the grid, the capacitance of capacitors can be reduced. However, in this case, the corresponding share of reactive power will be consumed within the grid, which cannot be considered reasonable.

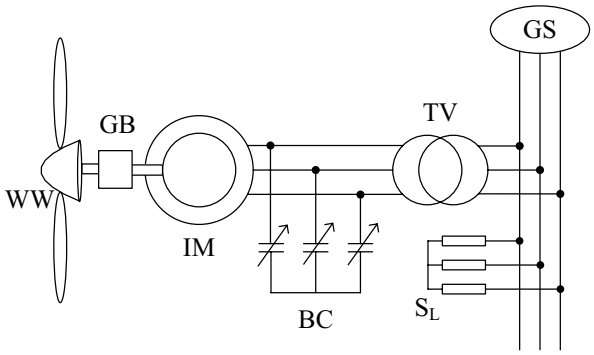

Figure 1. WTS with a SCIG and capacitor excited on the side of the stator: WW – wind wheel, GB – gear box, IM – induction machine, BC – bank of capacitors, TV – transformer, GS – generating system, S_L – load.

2.2 WTS with a SCIG and active rectifier

The disadvantage of the previous type, arriving from the use of adjustable capacitors for self-excited IM, can be eliminated by using a low-distorting 3-phase rectifier - LDTR (otherwise an active rectifier or converter), operating in the reactive power compensator mode - RPC [8,9,10,11,12] - Fig.2. In this type, it is possible to ensure the return of IM to the grid not only as the active power, but also (partially) to compensate the reactive power in the grid. The possibility of implementing this option is obvious, but information on the finding of research has yet been revealed. It can be assumed that there may be problems with the dynamic stability of the IM operation (for drafts and load shedding). However, in principle, this consideration is determined by the concept of building a control system (CS) - how fast it will be. The shortcomings of this structure should also include the already mentioned incomplete (50%) utilization of the power of the wind wheel.

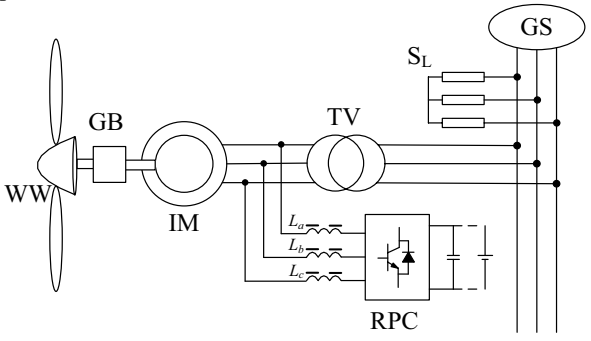

Figure 2. WTS with a SCIG and excitation from an electronic reactive power compensator – RPC: L_j – mutual coupled inductors.

2.3 WTS with a SCIG and Full-scale Power Converter (FPC)

It is possible to eliminate the first predicted deficit by complicating the power part of the generating system by introducing a three-phase voltage inverter - TVI - into it in addition to the LDTR, as shown in Fig.3 [3,13,14,15,16] These two power units, used together, functionally represent a full-scale power converter - FPC. If necessary, a matching transformer is installed at the output of the FPC. Dynamic modes here are largely damped by a buffer capacitor, included in the DC link between LDTR and TVI. LDTR works here in combined mode - in the mode of the LDTR and in the RPC mode, and TVI - in the mode send into the grid only active power from stator wound. The disadvantage of this solution is the need of relatively large rated power of the FPC (equal to the IM power) and also the 50% use speed band of the wind wheel, arising from the inability of transmitting rotor active power to the grid while in the mode of super-synchronous.

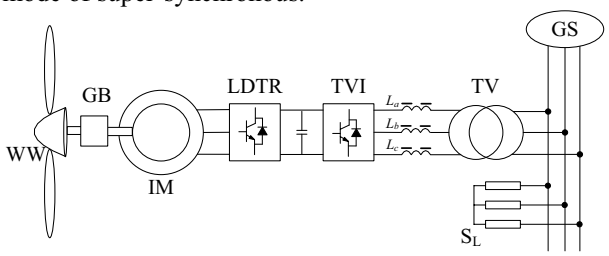

Figure 3. WTS with a SCIG and full-scale power converters: converter-1 (LDTR mode), converter-2 (TVI mode) is connected directly to the grid.

2.4 WTS with a doubly-fed induction generator (DFIG) and Power converter

In these variants structural of WTS, the wires from the rotor coil are attached to slip rings. In this case, two basic structures are possible.

The first structure is charractised by the sequential combination of rotor winding, power converter, stator winding and the connection of this whole circuit to the grid. It is described, for example, in [17, 18]. However, we could not find out information that needed in order to make a comparative evaluation of this structure with other alternative options, which is necessary at the engineering design stage. However, based on a simple analysis of this solution, we have noted the following shortcomings. Since the fundamental elements of the power converter is the rotor winding, therefore, the slip rings of the IM must be designed for the same current as the stator winding. This means the rotation ratio between the rotor and stator windings must be specially coordinated at the design stage. When performing the power converter in the form of two converter (converter-1 and converter-2), careful consideration should be given to the physical processes in the DFIG and the concept of controlling the converter-1 and converter-2, especially in the mode of sub-synchronous speed, when the rotor windings consumes the active component of the current, and the stator winding provides only active current into

the grid. Maybe this structure can only work in the mode of hyper- synchronous speed.

In the second variant of WTS, the rotor and stator circuits are not directly connected – instead the rotor windings together with the power converter forms a separate circuit that is connected to the grid – Fig 4.

Power converter is then connected to the rotor winding and the grid either directly or through a matching transformer.

Such a solution makes it possible to use the energy of the rotor in hyper-synchronous speed in a useful way by putting it into the grid and there by doubling the utilization factor of the wind wheel. To denote this structure, two terms are used: wound rotor induction generator (WRIG) and doubly-fed induction generator (DFIG). Here the second notation is used. A variant of the wind turbine is shown in Fig. 4 [2,5,19]. Formally, the same power converter structure is used here, as in Fig. 3, but power converter is installed here in a less powerful circuit. Since each of the converter (referred to above as LDTR and TVI), depending on the speed range, should operate in different modes (rectifier and inverter), then it would be convenient to refer them to more general term - abbreviations - back to back converters - converter-1 and converter-2. This type WTS is the most complex both in terms of power signal and information, but it is energetically most effective and potentially should be more stable in dynamic modes. The disadvantages include the presence of slip rings, which to eliminate require solving the problem of ensuring non-contact.

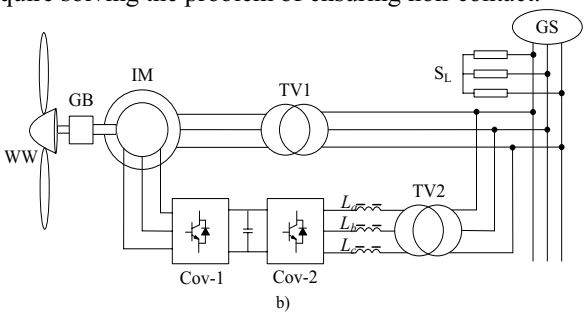

Figure 4. WTS based on doubly-fed induction generator - DFIG with self-excited from the rotor.

2.4.1 Features of power converters operation in the first and second speeds zones

In this paper, the WTS (see Fig. 4) is connected directly to the grid generated only active power.

Compensation of the IM stator's reactive power in both zones is ensured by the converter-1 by supplying the rotor winding with a voltage of the slip speed $f_r=sf_s$, where f_s – the stator frequency is fixed if the stator is connected directly to the grid; f_r – the frequency of the rotor voltages and currents and in the first zone (for $s>0$) with sequential phase alternation, and in the second zone ($s<0$) with the inverse. In sub-synchronous speed, the converter-1 through the converter-2 uses only the active power from the grid and operates in the TVI mode, and in hyper-synchronous speed - in the LDTR mode. In both zones, the value of the phase angle $\varphi_{r(1)}$ of the rotor current relative to its phase voltage (in terms of fundamental harmonics) is determined in the condition that only active power from stator into the grid is generated. This loop is controlled by the parameters μ_1 and θ_1 (where μ_1 is the modulation index PWM, and θ_1 is the load angle [13-15]).

The converter-2 is in sub-synchronous speed operation in the LDTR mode (with the parameters μ_2 and θ_2), which ensures the consumption of only active power only from the grid. In hyper-synchronous speed operation, the converter-2 operates in the TVI mode is connected directly to the grid (with the corresponding values of the parameters μ_2 and θ_2, which ensure return of only active power of the rotor to the grid).

The power converter depends on the speed range of the drive shaft. For example, with the slip range of $s\approx\pm0.3$, in the example considered here the speed multiplication $K_n=n_{max}/n_{min}=(1+0.3)/(1-0.3)=1.85$, corresponds to, the installed (full) power of the converter-1 from the installed capacity of the stator of the DFIG is – $P_{Cov1}\approx P_{Cov2}\approx 0.3P_s$. On the other hand, results of computer simulation showed that, the active power consumed by the rotor from the grid in sub-synchronous speed operation and the active power that delivered to the grid in hyper-synchronous speed operation are practically the same and equal to $P_r\approx 0.3P_s$. Thus, in sub-synchronous speed, the IM stator supplies operating power to the grid, minus the power consumed by the rotor for self-excitation, and in hyper-synchronous speed, the active power of the rotor is also added to the grid in addition to the stator power.

Taking the above into account, we can make a useful conclusion for the system design of a WTS: if the speed of the wind flow varies significantly, having mechanical or electromechanical means for stabilization of the shaft rotation wind wheel, for example, in the form of a gear box (GB in Fig. 1) changes in the slip speed and, accordingly, will reduce the rated capacity power (and cost) of power converters.

2.4.2 Concept synthesis control system of power converter for WTS

Synthesis of the control system (CS) is defined by the functional tasks described above, which need to be solved in 2 speeds zones. Recall that in sub-synchronous speed, the converter-1 operates in the TVI mode and the converter-2 operates in the LDTR mode; in hyper-synchronous speed, the converter-1 operates in the LDTR mode, and the converter-2 in the TVI mode. The fundamental important elements that determine the operation of the converter-1 and converter-2 in the two modes are filter with inductances - L_{1j} and L_{2j} (j = *a, b, c* - the phase index) placed at their outputs in each phase. In converter-1, these elements are the leakage inductances of the rotor winding. If necessary, additional L_{1j} can be introduced here. For the converter-2, the rational value of the parameter L_{2j} must be determined. In the context of this paper, a clear solution of this problem is not given, since it depends on the specified design criteria. Obviously, to reduce the distortion of the current that flows into the current grid, the matching inductance or the carrier frequency of the converter-2 must be increased.

An improper increase in the value of the parameter L_{2j} leads to an increase in the back-EMF of the converter-2, and voltage level across its component.

To explain the basic procedure that synthesis the control system of converter-1 and converter-2, we assume that the inductive resistance L_{2j} converter-2 is much larger than the equivalent resistance of its windings: $X_{L2j}>>R_{L2j}$ (with allowance for loss in its magnetic circuit showed in the coil) and use method described in [13,14].

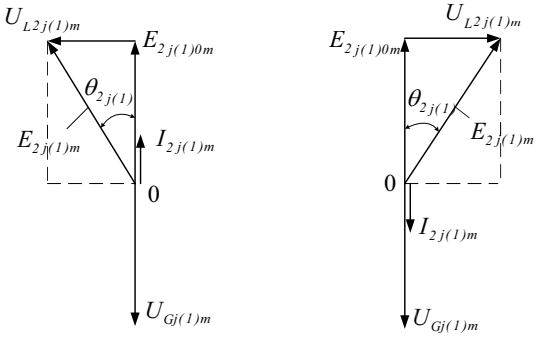

Figure 5. Phasor diagrams explaining the processes in the converter-2 (in terms of the fundamental harmonic) in two modes: a) - in the TVI mode connected directly to the grid; and b) - in the LDTR mode
$U_{Gj(1)m}$ – voltage *j*-phase of the grid; $E_{2j(1)0m}$ – back-EMF of converter-2 at idle; $E_{2j(1)m}$ – back-EMF in the mode of recoil into the grid an active current; $I_{2j(1)m}$ – active current send to the grid; $\theta_{2j(1)}$ – the load angle; $U_{L2j(1)m}$ – the voltage drop across the inductor L_{2j}.

Then, to determine the required values of the parameters μ_2 and θ_2 for controlling the converter-2, we can use the phasor diagrams shown in Fig. 5. They are built, example, for the mode of recoil into the grid an active power (see Fig. 5a) as follows: knowing the value of the current $\dot{\mathbf{I}}_{\mathbf{2j(1)m}}=\dot{\mathbf{I}}_{\mathbf{L2j(1)m}}$, given to the grid whose vector is opposite to the grid voltage vector $\dot{\mathbf{U}}_{\mathbf{Gj(1)m}}$, we find the voltage drop $\dot{\mathbf{U}}_{\mathbf{L2j(1)m}}$ on L_{2j} whose vector is orthogonal to the vector of its current $\dot{\mathbf{I}}_{\mathbf{L2j(1)m}}$ and collinear with its back-EMF vector – $\dot{\mathbf{E}}_{\mathbf{2j(1)0m}}$ in converter-2 idle mode. In the general mode, the vectors $\dot{\mathbf{U}}_{\mathbf{Gj(1)m}}$ and $\dot{\mathbf{E}}_{\mathbf{2j(1)0m}}$ are in anti-phase. We find the required parameters of the back-EMF vector converter-2 $\dot{\mathbf{E}}_{\mathbf{2j(1)m}}$ by connecting end of the vector $\dot{\mathbf{U}}_{\mathbf{L2j(1)m}}$ from the origin 0. Knowing values of $\dot{\mathbf{E}}_{\mathbf{2j(1)0m}}$ and $\dot{\mathbf{E}}_{\mathbf{2j(1)m}}$, we find the parameter $\mu_2=|\dot{\mathbf{E}}_{\mathbf{2j(1)0m}}|/|\dot{\mathbf{E}}_{\mathbf{2j(1)m}}|$. The load angle θ_{2j} is determined from a right-angled triangle:

$$\theta_{2(1)}j=arctg(|\dot{\mathbf{U}}_{\mathbf{L2j(1)m}}|/|\dot{\mathbf{E}}_{\mathbf{2j(1)0m}}|) \quad (2)$$

The values of the parameters μ_2 and $\theta_{2(1)j}$ found here are used to control the converter-2. The accepted assumption may give a slight deviation from the ideal result, which, however, can be eliminated by appropriate adjustment (in manual or automatic mode). This simplified procedure for determining parameters μ_2 and $\theta_{2(1)j}$ is the basis for the synthesis of the control system of converter-2.

For converter-1, the task of determining parameter μ_1 and $\theta_{1(1)j}$ becomes more complicated because here the frequency of the rotor voltage is changed from $f_r=0$ to $f_r=sf_s$, the active resistance of the rotor winding becomes commensurate with the inductance and must be taken into account. However, the essence of the methodology for solving the problem, for this case, remains the same.

Thus, the problem of synthesis of CS-1 and CS-2 for converter-1 and converter-2 is essentially reduced to the determining two control parameters μ_1, $\theta_{1(1)j}$ and μ_2, $\theta_{2(1)j}$, provided that only the given level of active power is generated into the grid. The problem formulated in this way determines the list of necessary functional nodes CS-1 and CS-2 and the required logic of their interaction. CS-1 and CS-2 should contain:

- Sensors of phase voltages of stator and rotor windings (their fundamental harmonics);
- Sensors of the phase currents of the stator and the rotor circuit (their fundamental harmonics), and in the rotor circuit the meters of two currents: the total current in the rotor winding and its active component, given to the converter-2;
- Phase discriminator of the angles $\varphi_{s(1)}$, $\varphi_{g(1)}$, i.e. angle sensors of the phase currents (their first harmonics) of the stator ($\varphi_{s(1)}$) and rotor fed to the grid ($\varphi_{g(1)}$) (at $s<0$), relative to their voltages (first harmonics); we recall that for $s<0$, the converter-2 should also consume only the active current from the grid;
- Two pulse width modulators (PWM-1, PWM-2), providing the formation of sinusoidal currents in the rotor winding and delivered by the rotor to the grid (through converter-2);
- Two phase loop lock control (PLL-1, PLL-2) for converter-1 and converter-2, providing a phase shift of the reference signal $u_{1refj}(t)$, $u_{2refj}(t)$ for PWM-1 PWM-2 (and accordingly rotation of the vectors back-EMF converter-1 and converter-2) at the required angles $\varphi_{s(1)}$, $\varphi_{g(1)}$;
- Two negative feedback circuit (NFC-$\varphi_{s(1)}$ and NFC-$\varphi_{g(1)}$), providing the generation of the newly active power grid by automatically tracking the equality $\varphi_{s(1)}=\pi$ and $\varphi_{g(1)}=\pi$ (when hyper-synchronous speed) or $\varphi_{g(1)}=0$ (when sub-synchronous speed);
- A loop of negative feedback on the voltage level of the stator (NFC-U_{sj}), but in fact by the level of the excitation current (in the winding of the rotor);
- Computing device.

The computer model of control system DFIG using all above listed components and operates in the mode that send to the grid only active power in the range of given sub-synchronous speed, for example, in [20] (without converter-2, and battery in place of DC-link capacitor).

3 Computer simulation results

The above are comparative analysis of different types of WTS base on DFIG - in Fig. 4 (in accordance with the term proposed in [15]) which based on earlier studies in the MATLAB/Simulink software environment [20]. With computer simulation, the mathematical model of DFIG was presented in [19,21].Note that the distortion of the current of the stator winding is determined by the rotor winding current distortion, which in turn are determined

by the carrier frequency ofconverter-1 and the inductance of the rotor.

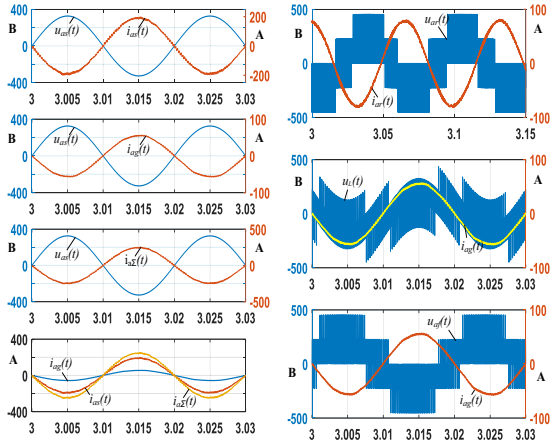

Figure 6. Generator operation of a 160 kVA DFIG at hyper-synchronous speed with s=-0.3, T_{em}=-612 N.m (electromagnetic torque) at f_c = 4kHz (carrier frequency):
$u_{as}(t)$ – the stator line voltage of phase a; (U_{as} = 230.9 B);
$i_{as}(t)$ – the stator current of phase a; ($I_{as(1)}$=135 A, THD_{Ias}=3.19%, $\varphi_{s(1)}$=180.3°);
$i_{ag}(t)$ – the output current of phase a of converter-2, ($I_{ag(1)}$=39.87A, THD_{Iag}=2.51%, $\varphi_{g(1)}$=180°);
$i_{a\Sigma}(t)$ – the total current of the wind turbine fed to the phase a grid; ($I_{a\Sigma(1)}$ = 174.9A, $THD_{Ia\Sigma}$=2.56%; φ=180.3°);
$u_{ar}(t)$ – the rotor voltage of phase a; ($U_{ar(1)}$=210.3 B);
$i_{ar}(t)$ – the rotor current of phase a; ($I_{ar(1)}$=55.76A, THD_{Iar}=2.75%)
$u_L(t)$ – the filter voltage; ($U_{L(1)}$=62.26 B);
$u_{af}(t)$ – the back-EMF of converter-2 of phase *a;* ($U_{af(1)}$=239,3 B);

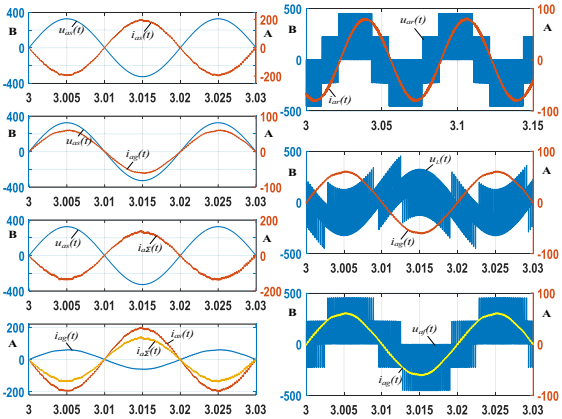

Figure 7. Generator operation of a 160 kVA DFIG at sub-synchronous speed with s=0.3, T_{em}=-612 N.m at f_c = 4kHz:
$u_{as}(t)$ – the stator line voltage of phase a; (U_{as} = 230.9 B);
$i_{as}(t)$ – the stator current of phase a; ($I_{as(1)}$=136.1A, THD_{Ias}=2.47%, $\varphi_{s(1)}$=180.2°);
$i_{ag}(t)$ – the output current of phase a of converter-2, ($I_{ag(1)}$=42.24A, THD_{Iag}=2.28%, $\varphi_{g(1)}$= 0°);
$i_{a\Sigma}(t)$ – the total current of the wind turbine fed to the phase a grid; ($I_{a\Sigma(1)}$=93.9A, $THD_{Ia\Sigma}$=3.76%; φ=180.3°);
$u_{ar}(t)$ – the rotor voltage of phase a; ($U_{ar(1)}$=217.6 B);
$i_{ar}(t)$ – the rotor current of phase a; ($I_{ar(1)}$=56.16 A, THD_{Iar}=2.59%);
$u_L(t)$ – the filter voltage; ($U_{L(1)}$=66,77 B);
$u_{af}(t)$ – the back-EMF of converter-2 of phase *a;* ($U_{af(1)}$=240,3 B);

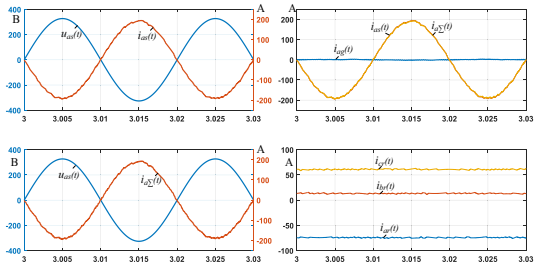

Figure 8. Generator operation of a 160 kVA DFIG at synchronous speed with s=0, T_{em}=-612 N.m at f_c = 4kHz:
$u_{as}(t)$ – the stator line voltage of phase a; (U_{as} = 230.9 B);
$i_{as}(t)$ – the stator current of phase a; ($I_{as(1)}$=135.6 A, THD_{Ias}=1.53%, $\varphi_{s(1)}$=180.2°);
$i_{ag}(t)$ – the output current of converter-2 of phase a, ($I_{ag(1)}$=1.02A, THD_{Iag}=86.97%, $\varphi_{g(1)}$= 4.8°);
$i_{a\Sigma}(t)$ – the total current of the wind turbine fed to the phase a grid; ($I_{a\Sigma(1)}$ = 134.5A, $THD_{Ia\Sigma}$=1.71%; φ=180.3°);
$i_{ar}(t)$, $i_{br}(t)$, $i_{cr}(t)$ – the rotor current of phase *a,b,c;* (I_{ar0}=-74.30 A; I_{br0}=13.27 A; I_{cr0}=61.03 A).

As the current distortions supplied to the grid by the rotor through conveter-2 have already been mentioned, therefore in this computer model, the inductance is L_{2j}=5mH.

In the study, all the parameters IM (power 160 kVA) are taken from [18]. The results of the computer model for DFIG are also presented in [18], but only in the sub-synchronous speed mode (s>0), which allowed to compare these known results with those obtained in the work. Their high coincidence (not worse than 2÷3%) is established. In this paper we also obtain the necessary results for the hyper-synchronous speed (s<0).

The oscillograms presented in Fig. 6 to Fig. 8 confirm the adequacy of modeling processes to the real processes. We note the principal difference in the phase position of the rotor current relative to its voltage in different operation modes of the IM. The lag of the rotor winding $i_{ar}(t)$ from its voltage $u_{ar}(t)$ by the angle φ_{ra}> π/2 at s<0 (see Fig. 6) indicates that its active component is in anti-phase with the rotor voltage, i.e. the rotor gives power to the grid, and the reactive power, providing the excited IM, lags by an angle of π/2. The sum of these two components gives the above-mentioned resultant current $i_{ar}(t)$. In another mode of s>0 (Fig. 7), active component of rotor current is already in-phase with its voltage, i.e. the rotor consumes (through converter-2) power from the grid. The sum of these components gives the resultant current $i_{ar}(t)$, which lags behind the voltage by an angle φ_{ra}<π/2. In the third mode, when s=0 (Fig. 8) in the winding of the rotor, currents $i_{ar}(t)$, $i_{br}(t)$, $i_{cr}(t)$are determined by small constant DC voltages that are provided by the converter-1. The power required to excite the IM, however, is negligible (about 600 W). The current consumed from the grid is also not significant, since it is consumed from the voltage source which is much greater than the voltage on the rotor windings. Further description of the oscillogram is superfluous, since there are all necessary explanations in the captions.

It is advisable to draw the attention of new technology developers to the great in formativeness of bringing oscillograms in the transmission (within the scope of publications) of new information, from which an adequate idea of physical processes required for an competent engineering design is created.

4 Conclusion

Systematized and make comparative evaluations variant uses of the squirrel-cage induction generator (SCIG) and doubly-fed induction generator (DFIG) for wind turbine system at qualitative level are necessary at the preliminary design stage (when determine the most suitable solution for given technical problems).

On the basic of computer simulation, the ability of DFIG with back to back converter connected with the rotor windings (in the form of two connected 2-level voltage source converters - converter-1 and converter-2) is confirmed at a variable speed of the drive shaft and when directly connected into the grid to give it: in the mode of $s<0$, the active power of the stator and rotor windings; and in the mode of $s>0$ - only by the stator windings. When $s>0$, the rotor winding does not recoil, but consumes active power from the network.

Obviously, in term of mass-size and energy indicators, the structure of DFIG (shown in Fig. 4) is the best among the considered variants, since in the slip range-$0.3<s<0.3$, the power converter in the rotor circuit is approx. 3 times smaller than the full power converter in the variant shown in Fig 3.

In range of the slip variation $-0.3<s<0.3$, corresponding to the speed multiplication $K_n=n_{max}/n_{min}=1.85$, the reduction ratio of the gear box can be either significantly reduced.

DFIG has existing defect due to the presence of slip ring within its structure.

References

1. E. Hau, *Wind Turbines: Fundamentals, Technologies, Application, Economics*, 2nd edition, Springer, 2005.
2. Ackermann T., *Wind Power in Power Systems*, John Wiley & Sons, Ltd, New York, NY, USA, 2005. 745 p.
3. Bin Wu, Yongqiang Lang, Navid Zargari, Samir Kouro (2011) *Power Conversion and Control of Wind Energy Systems*, Aug 2011, Wiley-IEEE Press, 480 p.
4. Bezrukikh P.P. *Wind power (reference and technical manual)* – Moscow: "Energia", 2010, 320 p.
5. Yongsu Han, Sungmin Kim, Jung-Ik Ha, and Wook-Jin Lee. *A Doubly Fed Induction Generator Controlled in Single-Sided Grid Connection for Wind Turbines* / IEEE Transactions on Energy Conversion, vol., 28, No.2, pp.412÷424, june 2013.
6. Toroptsev N.D. *Aircraft asynchronous generators*. - Moscow: Transport, 1970. - 204s.
7. Petrov G.N. *Electric machines, p.2. Asynchronous and synchronous machines*. M.-L.: Gosenergoizdat, 1963. - P.416s.
8. Goryakin D.V, Mytsyk G.S. *Three-phase bridge inverter circuit in the mode of the reactive power compensator*. Practical power electronics, 2012, No. 45. - p.13 ÷ 17.5.
9. Viriya P, Matsuse K. *Low-harmonic GTO converter for fundamental power factor compensation*. IEEE Trans Power Electron 1991; 6:371–9.
10. Ooi B-T, Dai S-Z. *Series-type solid-state static VAR compensator*. IEEE Trans Power Electron 1993; 8:164–9.
11. Harley R, Rigby B, Jennings G. *Design of a controlled converter which emulates a series capacitive compensator for long power lines*. Proc. int. conf. power electronics and motion control (PEMC'94); 1994. p. 213–8.
12. Joos G, Moran L, Ziogas P. *Performance analysis of a PWM inverter VAR compensator*. IEEE Trans Power Electron 1991;6:380–91.
13. Goryakin D.V, Mytsyk G.S. *Research of operating modes of the three-phase bridge inverter circuit*. - Electricity, 2012, No.5, p.23 ÷ 31.
14. Mytsyk G.S, Goryakin D.V. *Non-contact machine-electronic generating system based on an asynchronous machine and an active rectifier*. Practical Power Electronics, 2018, No. 69. p. 45 ÷ 49.
15. Mytsyk G.S, Myo Min Thant. *The system design problem of the electrotechnical complex "Variable speed - constant frequency"*. Electricity, 2018, No. 2. - p.34 ÷ 42.
16. Kio Zaw Lin., *Research of possibilities of improvement of quality indicators of autonomous system of generation of voltage of stable frequency on the basis of the synchronized asynchronous generator*, Thesis - MPEI, Moscow-2012.
17. Berilov A.V, Eremenko V.G., Nguyen Huu Nam, *Investigation of a wound rotor induction generator with stator and rotor windings connected in series through a frequency converter,* Vesnik MPEI, №4/2016, 56-61 p.
18. Eremenko V.G., Berilov A.V, Nguyen Huu Nam, The patent of Russian Federation for utility model No. 151665. "Asynchronized synchronous generator." Posted on 10/04/2015 Bulletin. № 10.
19. G. Abad, J.S. Lopez, M.A. Rodrıguez, L. Marroyo, and G. Iwanski, *Doubly fed induction machine: Modeling and control for wind energy generation*: Wiley, 2011.
20. Herman-Galkin. S.G. *Virtual laboratories of semiconductor systems in MATLAB/Simulink*: Textbook. - SPb.: Publishing House "Lan", 2013. - 448 p.
21. Kopylov I.P. *Mathematical modeling of electric machines*: Proc. for high schools. Moscow: "High School" 2001, 327 p.